Bioactive Materials 29 (2023) 36–49

Contents lists available at ScienceDirect

Bioactive Materials

journal homepage: www.keaipublishing.com/en/journals/bioactive-materials

Microvascular endothelial cells derived from spinal cord promote spinal cord injury repair

Zhifeng You [a,1], Xu Gao [a,b,1], Xinyi Kang [c], Wen Yang [a], Tiandi Xiong [a,d], Yue Li [e], Feng Wei [a,d], Yan Zhuang [a,d], Ting Zhang [e], Yifu Sun [b], He Shen [a,d,**], Jianwu Dai [a,f,*]

[a] Key Laboratory for Nano-Bio Interface Research, Division of Nanobiomedicine, Suzhou Institute of Nano-Tech and Nano-Bionics, Chinese Academy of Sciences, Suzhou, 215123, China
[b] Department of Orthopaedic Surgery, China-Japan Union Hospital of Jilin University, Changchun, 130033, China
[c] Department of Obstetrics and Gynecology, The Second Affiliated Hospital of Soochow University, Suzhou, 215004, China
[d] School of Nano-Tech and Nano-Bionics, University of Science and Technology of China, Hefei, 230026, China
[e] i-Lab, Key Laboratory of Multifunction Nanomaterials and Smart Systems, Suzhou Institute of Nano-Tech and Nano-Bionics, Chinese Academy of Sciences, Suzhou, 215123, China
[f] State Key Laboratory of Molecular Developmental Biology, Institute of Genetics and Developmental Biology, Chinese Academy of Sciences, Beijing, 100101, China

ARTICLE INFO

Keywords:
Microvascular endothelial cells
Spinal cord injury
NeuroRegen scaffold
Neural regeneration

ABSTRACT

Neural regeneration after spinal cord injury (SCI) closely relates to the microvascular endothelial cell (MEC)-mediated neurovascular unit formation. However, the effects of central nerve system-derived MECs on neovascularization and neurogenesis, and potential signaling involved therein, are unclear. Here, we established a primary spinal cord-derived MECs (SCMECs) isolation with high cell yield and purity to describe the differences with brain-derived MECs (BMECs) and their therapeutic effects on SCI. Transcriptomics and proteomics revealed differentially expressed genes and proteins in SCMECs were involved in angiogenesis, immunity, metabolism, and cell adhesion molecular signaling was the only signaling pathway enriched of top 10 in differentially expressed genes and proteins KEGG analysis. SCMECs and BMECs could be induced angiogenesis by different stiffness stimulation of PEG hydrogels with elastic modulus 50-1650 Pa for SCMECs and 50-300 Pa for BMECs, respectively. Moreover, SCMECs and BMECs promoted spinal cord or brain-derived NSC (SNSC/BNSC) proliferation, migration, and differentiation at different levels. At certain dose, SCMECs in combination with the NeuroRegen scaffold, showed higher effectiveness in the promotion of vascular reconstruction. The potential underlying mechanism of this phenomenon may through VEGF/AKT/eNOS- signaling pathway, and consequently accelerated neuronal regeneration and functional recovery of SCI rats compared to BMECs. Our findings suggested a promising role of SCMECs in restoring vascularization and neural regeneration.

1. Introduction

Spinal cord injury (SCI) has been described as an incurable disease for thousands of years and remains one of the most challenging medical problems [1], which resulted in devastating consequences of physical disability, psychological disorders, and social burdens for approximately 27 million patients and their families worldwide [2,3]. Injuries of the vascular system and the blood-spinal cord barrier (BSCB) are key events in SCI, triggering a cascade of pathological reactions that aggravate the impairment of the spinal cord [4,5]. The spatial and temporal abnormalities in BSCB permeability are also negatively correlated with motor function recovery [6–8]. The dysfunction of the neurovascular microenvironment is one of the major bottlenecks in spinal cord regeneration. Strategies, such as administration of pro-angiogenic factors [9–11],

Peer review under responsibility of KeAi Communications Co., Ltd.
* Corresponding author. Key Laboratory for Nano-Bio Interface Research, Division of Nanobiomedicine, Suzhou Institute of Nano-Tech and Nano-Bionics, Chinese Academy of Sciences, Suzhou, 215123, China.
** Corresponding author. Key Laboratory for Nano-Bio Interface Research, Division of Nanobiomedicine, Suzhou Institute of Nano-Tech and Nano-Bionics, Chinese Academy of Sciences, Suzhou, 215123, China.
E-mail addresses: hshen2009@sinano.ac.cn (H. Shen), jwdai@genetics.ac.cn (J. Dai).
[1] These authors contributed equally to this work.

https://doi.org/10.1016/j.bioactmat.2023.06.019
Received 4 April 2023; Received in revised form 6 June 2023; Accepted 23 June 2023
Available online 28 June 2023

genes therapy [12,13], and cell transplantation [14–16], have been developed to promote vascularization after SCI. However, the endogenous endothelial cell formed vessels are usually leaky and do not fully reestablish the BSCB nor provide sufficient support to the local metabolism. Therefore, there remains an urgent need to develop approaches for modulating the neurovascular system after SCI to enhance neural regeneration and functional restoration.

Microvascular endothelial cells (MECs), the major element of neurovascular system in the CNS, lay essential roles in the maintenance of the spinal cord and brain homeostasis, as well as in certain pathological conditions [17,18]. Damage and death of spinal cord endothelial cell (SCEC) plays a prominent role in secondary injury after SCI [19]. Similar to MECs in the spinal cord, brain-derived MECs (BMECs) are responsible for triggering brain tissue damage [20]. Transplantation of BMECs could ameliorate behavioral outcomes after in ischemic brain injury, suggesting a beneficial effect of the transplanted BMECs in modulation dysfunction of CNS. Furthermore, it was also reported that brain endothelial cell (BEC) as a critical component of the neural stem cell (NSC) niche in stimulating NSC renewal and neurogenesis [21]. The findings of BMECs nourishing nerves [22], as well as BEC-formed microvessels guiding axon growth in SCI model suggested that BEC intervention may also be a promising approach to SCI repair [23]. However, the effects of MECs, particularly derived from CNS, on neovascularization and neurogenesis after SCI, and potential signaling involved therein, are unclear. As Spinal cord-derived NSCs (SNSCs) and brain-derived NSCs (BNSCs) exhibited different efficiency in spinal cord reconstruction [24], it's hypothesized that SCMECs and BMECs, despite their functional similarity, might also differ in their effects on angiogenesis, the acceleration of neural differentiation and consequently, in SCI repair.

In this study, we aimed to uncover the different effects of CNS-derived MECs on SCI repair, particularly on regulating neovascularization and neuroregeneration through systematically comparing the characteristics of SCMECs and BMECs and examining their interactions with SNSCs and BNSCs, respectively (Fig. 1). We found that angiogenesis and cell adhesion molecular signaling-related genes and proteins were differentially expressed in SCMECs compared to that in BMECs by transcriptomic and proteomic profiling. SCMECs and BMECs could acquire the angiogenic phenotype in response to specific elastic modulus of hydrogels and promoted the proliferation, migration, and neural differentiation. Furthermore, we investigated the effects of SCMECs or BMECs intervention in the vascular niche and their therapeutic potential in a complete SCI rat model.

To improve cell retention and survival rates after transplantation in SCI animals, we combined them with biomaterial scaffolds [4,25,26]. The NeuroRegen scaffold was developed in our laboratory and used together with stem cells in clinical trials, successfully promoting autonomic neural function recovery, increases sensation level, and improves locomotor activity in patients with SCI [27,28].This scaffold not only support MEC growth at defect, but also provide a structural platform for axonal regeneration after SCI. After implantation of the SCMEC-laden NeuroRegen scaffold, the vascular reconstruction was significantly improved in a complete SCI rat model, synergistically accelerating neuronal regeneration and functional recovery compared to BMEC-loaded NeuroRegen scaffold implantation. We also investigated the underlying mechanisms of this approach. This work lays the foundation for further research toward the application of SCMECs for SCI therapy.

2. Materials and methods

2.1. Animals

6-8-week-old female and newborn Sprague-Dawley rats were purchased from Shanghai Slaughter Laboratory Animal Co (Shanghai, China). 6-8-week-old GFP-expressing transgenic Sprague-Dawley rats were a kind gift from the Institute of Genetics and Developmental Biology, Chinese Academy of Sciences. All animal experiments were approved by the Institutional Animal Care and Use Committee and conducted following the governmental and the Chinese Academy of Sciences guidelines for animal welfare (approval NO. SINANO/EC/2021-026).

2.2. Cells and culture media

Primary SCMEC, BMEC, GFP-SCMECs, and GFP-BMECs were isolated from Sprague-Dawley rats, and primary SNSCs and BNSCs were isolated from newborn-Sprague-Dawley rats. Primary endothelial cells were cultured using Endothelial Cells Culturing Medium (ECCM) based on DMEM/high glucose (4.5 g/L; Gibco) containing 10% fetal bovine serum (Gibco), 1% endothelial cells growth supplement (ScienCell), and 1%

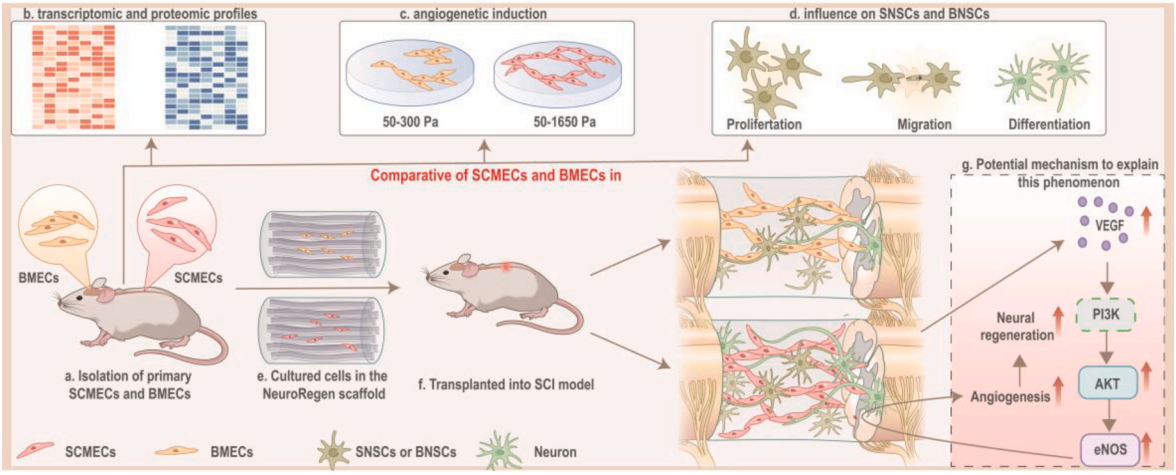

Fig. 1. Schematic of the project. (**a and b**) SCMECs/BMECs isolation were established to systematically compare differences between SCMECs and BMECs in transcriptomic and proteomic profiles. (**c**) It was inferred by transcriptomic/proteomic profiles and validated through PEG hydrogels with different elastic modulus that angiogenetic activity in SCMECs and BMECs were different. (**d**) It was also proved that the proliferation, migration, and differentiation of neural stem cells, which was essential for spinal cord injury repair, was promoted by SCMECs or BMECs, suggesting SCMECs/BMECs benefit angiogenesis and neuron regeneration for spinal cord repair. (**e to g**) In combination with NeuroRegen scaffold, SCMECs showed higher effectiveness in the promotion of vascular reconstruction through the VEGF/AKT/eNOS- signaling pathway than BMECs, and consequently accelerated neuronal regeneration in spinal cord injury rats. SCMECs, spinal cord microvascular endothelial cells; BMECs, brain microvascular endothelial cells.

penicillin-streptomycin and supplemented or not with puromycin for selection. Primary SNSCs and BNSCs were cultured in a proliferation medium (DMEM/F12 containing 20 ng/mL bFGF, 20 ng/mL EGF, and 2% B27) or differentiation medium (DMEM/F12 containing 2% B27). All cells were maintained at 37 °C in an incubator with an atmosphere with 5% CO2 and 95% O2.

2.3. Isolation of primary SCMECs and BMECs

Rats were anesthetized by intraperitoneal injection of pentobarbital sodium, and spinal cord and brain tissues were immediately dissected and immersed in calcium- and magnesium-free Hank's balanced salt solution (HBSS; Solarbio) pre-cooled at 4 °C. After the removal of outer membranes and big vessels, spinal cord tissues were cut with sterilized scissors and homogenized in a specially designed tissue grinder based on the Dounce tissue grinder, whereas brain tissues were homogenized to a uniform suspension with the sequential use of 25 mL, 10 mL, and 5 mL serological pipettes (Corning). The tissue homogenates were transferred to 50 mL sterile centrifuge tubes and centrifuged at 4 °C, 3000×*g* for 5 min; the pellet was resuspended in 20% bovine serum albumin (BSA) (in calcium- and magnesium-free HBSS) and centrifuged again at 4 °C, 3000×*g* for 15 min. The precipitated microvessel segments were washed with HBSS, digested with 2 mg/mL collagenase IV (Gibco) and 50 μg/mL DNase (Sigma) in Dulbecco's modified Eagle's medium (DMEM) at 37 °C for 1–2 h, centrifuged at 500×*g* for 7 min to terminate the digestion, resuspended in Endothelial Cell Culture Medium (ECCM), and seeded into cell culture flasks pre-coated with collagen (Biocoat; 100 or 500 μg/mL in 0.02 N acetic acid at 37 °C overnight) and/or fibronectin (Sigma; 5 or 30 μg/mL in sterile deionized water at 37 °C for at least 4 h). After 1–2 days, the medium was replaced with fresh ECCM supplemented with puromycin (Beyotime, China) at the concentration of 800 ng/mL to remove contaminating cells; once SCMECs and BMECs reached 80–95% confluence, they were subcultured.

2.4. Isolation of SNSCs and BNSCs

SNSCs and BNSCs were isolated from spinal cord and brain of newborn rats [29]. Briefly, after collecting spinal cord and brain tissues, meninges were stripped away from the tissues. And then the tissues were cut into pieces and digested in TrypLE (Thermo) for 15 min at 37 °C to obtain cell suspension. Cells suspension were diluted with phosphate-buffered saline (PBS) and centrifugated at 1000 rpm for 5 min. The precipitate was resuspended in NSC proliferation medium and seeded on a cell culture plate. Half of the medium was replaced with the fresh one every three days until newly formed neurospheres were obtained.

2.5. Immunostaining

Cells staining was performed according to the following protocol: Cells were fixed with 4% paraformaldehyde (PFA; Leagene, Beijing, China) for 15 min, washed with PBS for three times, and permeabilized with 0.5% Triton (Sigma) for 10 min. After three times of PBS washing, samples were blocked with 5% BSA for 1 h and incubated with primary antibodies (Supplementary Table 1) at 4 °C overnight. After incubation with secondary antibodies at 1:500 dilution and DAPI at 1:1000 dilution for 1 h at room temperature, cells were observed under an Olympus FV3000 laser scanning confocal microscope.

2.6. Flow cytometry

SCMECs and BMECs were collected, fixed with 2% PFA for 15 min, and washed with PBS. Then, cells were stained with primary antibodies (Table S1) for 1 h and washed with PBS. After incubation with secondary antibodies for 1 h and washed with PBS, the cells were resuspended in PBS, and at least 10,000 cells per sample were analyzed on FACSC elesta (BD Biosciences).

2.7. RNA-seq and data analysis

Total RNA was extracted from SCMECs and BMECs samples labeled SR1, SR2, SR3 and BR1, BR2, BR3, respectively, using TRIzol (Invitrogen), following the manufacturer's instructions. RNA was analyzed for quality and quantity using Agilent 2100 BioAnalyzer and the Qubit RNA assay kit (Invitrogen). High-quality RNA samples with RNA integrity number (RIN) >7.0 and a 28S:18S ratio >1.8 were used for library construction using CapitalBio Technology Inc. (Beijing, China) with the Ultra RNA Library Prep Kit for Illumina (NEB). After final libraries quantification using KAPA Library Quantification Kit (KAPA Biosystems, South Africa) and validation through reverse transcription-polymerase chain reaction (RT-qPCR) in Agilent 2100 Bio Analyzer, libraries were subjected to paired-end sequencing (150-base pair reads) on an Illumina NovaSeq sequencer (Illumina) by CapitalBio Technology Inc. (Beijing, China). (Beijing, China). GO terms and heatmaps were analyzed using an online bioinformatics tool (www.bioinformatics.com.cn) for data analysis and visualization.

2.8. Proteomics sequencing and data analysis

Protein extraction from SCMEC and BMEC samples labeled SP1, SP2, SP3 and BP1, BP2, BP3, respectively, was carried out using lysis buffer (8 M urea, 2 M thiourea, 4% CHAPS, 20 mM Tris-base, 30 mM dithiothreitol (DTT), 1 mg/10 μL) and protease inhibitors (Roche, Basel, Switzerland) on ice. Peptides were obtained using trypsin (sequencing grade) digestion, labeled with TMT Label Reagent and quenched with hydroxylamine, according to the manual of TMT Mass Tagging Kits and Reagents (Thermo Fisher Scientific, USA). Proteins were analyzed using the nanoscale liquid chromatography system U3000 nano (Thermo Fisher Scientific, USA) and the mass spectrometer Q-Exactive (Thermo Fisher Scientific, USA) at CapitalBio Technology Inc. Raw data analysis was processed using the Proteome Discoverer 2.3 software (Thermo Fisher Scientific, USA). Samples for RNA-seq and proteomics analysis were isolated from cells in the same culture passage.

2.9. Scanning electron microscopy

The NeuroRegen with SCMECs and BMECs or not were fixed by 2.5% glutaraldehyde for 2 h and then washed with 0.1 M PBS for three times. Dehydration was carried out in a gradient of 50%, 70%, 80%, 90%, 95%, and 100% ethanol. Samples were dried and then coated with gold for 120 s. Images were taken by Hitachi S-4800 scanning electron microscope.

2.10. Preparation of PEG hydrogels

PEGDA was a kind gift from Prof. Y. Du (Tsinghua University, Beijing, China). PEG hydrogel samples of different stiffness were prepared from 0.1% to –0.5%, 1%, and 2% PEGDA as previously reported [30].

2.11. Cell proliferation assay

The influence of SCMECs/BMECs on SNSC/BNSC proliferation was analyzed using transwell assays. SNSCs or BNSCs were seeded on the plates coated with 100 μg/mL of PDL at a density of 5×10^4 cells/well, whereas SCMECs or BMECs were placed into transwell inserts (Corning). After 3 days of culture, DNA synthesis was measured using the Beyo-Click™ EdU Cell Proliferation Kit with Alexa Fluor 488-coupled azide (Beyotime, China) following the manufacturer's protocol. Briefly, cells were labeled with 10 μM EdU for 6 h, fixed with 4% PFA for at least 15 min, and permeabilized with 0.5% Triton for 15 min at room temperature. After treatment with click reaction buffer for 30 min and staining with Hoechst 33342 at a dilution of 1:1000, proliferative cells labeled

with Alexa Fluor 488-azide were detected under an Olympus FV3000 laser scanning confocal microscope.

2.12. Migration assay

Neurospheres (SNSCs or BNSCs) were placed into on the bottom of transwell plates coated with PDL, co-cultured with SCMECs or BMECs for 24 h, and analyzed using phase-contrast microscopy (Nikon Eclipse 55i, Nikon). The distance of neural cell migration from the edge of the neurospheres was measured using the NIKON software.

2.13. SCMECs/BMECs cultured on NeuroRegen scaffold and characterization

4-mm sterilized NeuroRegen scaffold was immersed in deionized water (ddH_20) and then dried for at least 30 min in the cells culture bench. SCMECs/BMECs with the number of 0.25×10^6, 1×10^6, or 4×10^6 were respectively resuspended at 200 μL culturing medium and dropped onto the scaffold to incubate at the cell incubator at least 3 h, after adding fresh medium for 3 h incubating, the NeuroRegen with cells were transferred into new wells with fresh medium and cultured overnight for in vivo implantation. Before implantation, cells in combination with NeuroRegen were washed with PBS.

After 1 d and 3 d cells culturing in the NeuroRegen scaffold, cells were stained with LIVE/DEAD viability/cytotoxicity kit (Invitrogen, USA), alamarBlue cell viability assay agent (Solarbio, China), and Phalloidin (Yeasen, China) following the manufacturer's protocol. The biocompatibility [31] of NeuroRegen was also evaluated.

2.14. SCI model

Rats were fasted for 8–10 h prior to intraperitoneal injection of sodium pentobarbital (30 mg/kg) for anesthesia. Surgical exposure is performed at the T8-T10 segment of the rat's back, T9 vertebral plate was removed with occlusal forceps, and a 4-mm piece of the T8–T9 spinal cord region was excised. After bleeding was stopped with gelatin sponges (Xiangen, China), NeuroRegen scaffolds [32] loaded or not with SCMECs or BMECs were transplanted into the lesions to form a continuous spinal cord, and muscles (fascia) and skin were sutured in layers. The following eight experimental groups (N = 10 in every group) were compared: Sci, unloaded scaffold, and scaffolds loaded with different numbers of SCMECs or BMECs: 0.25×10^6 (SC. or BC.), 1×10^6 (SC1 or BC1), or 4×10^6 (SC4 or BC4).

2.15. Behavioral assessment

Motor function recovery in rats with SCI was assessed according to the Basso-Beattie-Bresnahan scale [33], which scores limb movement, paw placement, coordination, and gait from 0 (paralysis) to 21 (normal). To analyze the recovery of hind limb muscle strength at 8 weeks postoperatively, the hind limbs were hit and their strength was recorded with a micro-structured pressure transducer [34]. For the inclined toggle test, the rats were placed on a horizontal surface with a gradually increasing inclination angle, and the maximum angle at which they did not slip for 5 s was recorded [35]. Each animal was tested three times.

2.16. Histological analysis

Rats were anesthetized 10 days or 8 weeks post-surgery after behavioral tests, 4% PFA was injected intracardially for perfusion to collect 3-cm-long spinal cord segments including the lesion site, sequentially immersed in 15 and 30% sucrose, embedded in Tissue-Tek OCT compound at −80 °C, cut into 12-μm-thick sections using a Leica freezing microtome, and subjected to histological analysis after immunolabeling and hematoxylin-eosin and LFB staining as described previously [36,37]. Antibodies used for immunostaining are listed in Table S1.

2.17. Statistical analysis

Raw data were statistically analyzed using GraphPad Prism. The results are expressed as the mean ± standard deviation (SD). The difference between two groups was assessed using a *t*-test. The difference between more than 3 groups was assessed using ANOVA analysis; $p < 0.05$ was considered to indicate statistical significance.

3. Results

3.1. Establishment of primary SCMEC and BMEC isolation

Inspired by the currently existing methods to isolate primary SCMECs and BMECs, we established a system for primary SCMECs and BMECs isolation, which includes mechanical dissociation and one-step enzymatic digestion (Fig. 2A). Brain and spinal cord tissue homogenates were obtained using pipettes of different sizes or a specially designed tissue grinder inspired by the Dounce tissue grinder, respectively, and microvascular segments were collected through centrifugation. After enzymatic digestion and clearance of contaminate using puromycin treatment, the digested microvessels displayed a "beads-on-a-string" appearance, which was consistent with the observations of a previous study [38]. SCMECs and BMECs migrated out of the digested microvessles and proliferated to cell confluence within 5–7 days (Fig. 2B). In addition to the mechanical dissociation optimization for microvessels harvesting, cell culture flask was also utilized to improve cell yield by coating with collagen and/or fibronectin. The results indicated that cells proliferated better in the fibronectin- than in collagen-coated plates and that the highest proliferation rate was observed in the plates coated with both collagen and fibronectin (Fig. 2C), suggesting that collagen–fibronectin coating should be used to isolate microvascular-derived endothelial cells (MECs).

Previous studies demonstrated that to avoid the growth of other cell types, ensuring purity in the MECs culture, cells could be treated with a permeability glycoprotein (P-gp) substrate, such as puromycin [39,40]. Therefore, to increase cell purity we used puromycin, which eliminated non-endothelial αSMA- and desmin-positive cells in a concentration-dependent manner (Fig. 2D and Fig. S1). In previous studies, puromycin has been administered immediately after microvessels attachment on day 0 [41,42]. However, to maximize cell adhesion and improve the SCMEC/BMEC yield, we added puromycin 24–48 h after the attachment of microvessels; thus, contaminating cells were efficiently eliminated and the purity of the isolated SCMECs and BMECs reached 99.8% and 99.6% stained with vwF, respectively (Fig. 2E and F). Also, the isolated SCMECs/BMECs were further verified with high purity by staining with CD31 and αSMA (Fig. S2). After the optimization steps described above including mechanical dissociation, coating strategy, and administration timing of puromycin, it is found that SCMEC/BMEC yield is 2×10^6/rat, which was >20-times higher than that reported previously [43], supporting the successful establishment of an efficient and time-saving protocal for primary SCMEC and BMEC isolation with a high yield and purity.

3.2. SCMECs and BMECs exhibit different transcriptional profiles

To investigate transcriptional differences between primary SCMECs and BMECs, we performed RNA-sequencing (RNA-seq). Three biological replicates in each group (SR1–3 and BR1–3) exhibited a high correlation with an average Pearson's correlation coefficient >0.96 (Fig. S3). Differentially expressed genes (DEGs) analysis by volcano plot revealed 1048 up-regulated and 1241 down-regulated genes ($\log_2$ FC ≥ 1 or ≤ -1, respectively; *p-value* ≤0.05) in SCMECs compared to those in BMECs (Fig. 3A and Fig. S3). DEGs were clustered in a heatmap to highlight transcriptomic differences between SCMEC and BMEC samples (Fig. 3B).

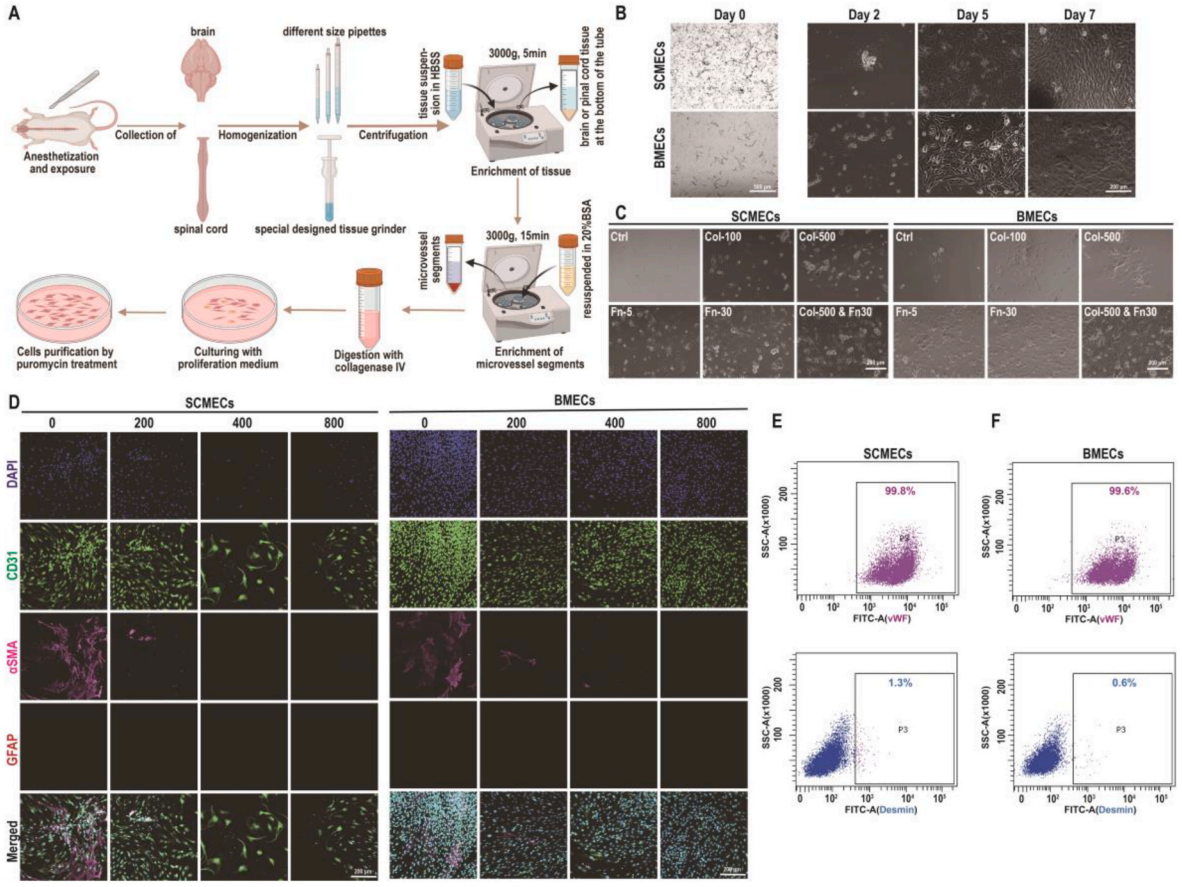

Fig. 2. Isolation and characterization of primary SCMECs and BMECs. (**A**) Schematic presentation of primary rat SCMECs and BMECs isolation procedure, SCMECs, spinal cord microvascular endothelial cells; BMECs, brain microvascular endothelial cells. (**B**) Morphology of SCMECs and BMECs after culturing for different indicated times, analyzed using phase contrast microscopy. Scale bars, 500 μm (day 0) and 200 μm (days 2–7). (**C**) Representative phase-contrast images of SCMECs (left) and BMECs (right) grown for 72 h on culture plates coated with 100 or 500 μg/mL collagen (Col) and/or 5 or 30 μg/mL fibronectin (Fn). Scale bar, 200 μm. (**D**) Representative immunofluorescence images of SCMECs (left) and BMECs (right) treated with the indicated concentrations of puromycin (ng/mL) and stained with DAPI (blue) and antibodies against CD31 (green), αSMA (pink), or GFAP (red). Scale bar, 200 μm. (**E** and **F**) Representative flow cytometry dot plots of isolated SCMECs (**E**) and BMECs (**F**) labeled with antibodies against vwF (upper panels) and desmin (lower panels).

In addition, top-ranked DEGs (Fig. S4) revealed that in SCMECs, homeobox (*HOX*) genes were strongly expressed and all of them had a higher expression level than that in BMECs (Fig. S5), which was consistent with a key role of *HOX* genes in determining endothelial cell positional identity and striking differences in *HOXB7* expression between SCMECs and BMECs observed in previous studies [44,45]. Kyoto Encyclopedia of Genes and Genomes (KEGG) pathway analysis revealed the DEGs enrichment mainly in the PI3K-AKT and cell adhesion molecule pathways, known to be involved in angiogenesis [46,47], followed by adhesion-related signaling pathways, such as ECM-receptor interaction and focal adhesion pathways, *etc* (Fig. 3C). Other enriched pathways were associated with neurogenesis-related signaling, including the axon guidance pathway, and immune-related pathways, such as leukocyte transendothelial migration, natural killer cell-mediated cytotoxicity, and systemic lupus erythematosus (Fig. 3C and Fig. S6), indicating that SCMECs and BMECs might be conditional immune cells in the BSCB and BBB. Gene Ontology (GO) term analysis revealed that DEGs were significantly enriched in system development and multicellular organismal development (biological process domain), plasma membrane part and extracellular space (cellular component domain), and protein binding and receptor binding (molecular function domain; Fig. 3D–F and Fig. S6).

3.3. Comparison of protein levels in SCMECs and BMECs

We also explored proteomics differences between SCMECs and BMECs to discover 288 up-regulated and 271 down-regulated proteins (FC $\geq$ 2 and $\leq$0.67, respectively; *p-value* $\leq$ 0.05) in SCMECs compared to those in BMECs (Fig. 4A). Cluster analysis of differentially expressed proteins (DEPs) and top 50 DEPs were also illustrated in heatmaps to reveal significant differences between SCMECs and BMECs (Fig. 4B and Fig. S7). The PANTHER classification system [48] revealed 15 and 12 protein classes in the up-regulated and down-regulated DEPs, respectively; among them, the class of metabolite interconversion enzymes ranked first, accounting for 18.2% and 43.9% of the upregulated and downregulated DEPs, respectively. Transporter, cytoskeletal, and membrane traffic proteins were special among the classification of down-regulated DEPs, whereas gene-specific transcriptional regulator proteins were specially associated with up-regulated DEPs (Fig. 4C).

To gain further insights into the functional role of DEPs, we performed GO and KEGG enrichment analyses. The GO analysis highlighted DEP enrichment in extracellular space, extracellular region, extracellular region part, cell surface, and immune-related events such as leukocyte cell-cell adhesion, leukocyte aggregation, antigen processing and presentation, and T cell activation (Fig. 4D). Additionally, 6 of 10 biological processes were related to immune-related processes (Fig. S8). KEGG pathway analysis indicated that 5 of the top 10 pathways were associated with metabolism-related pathways, and 2 categories related

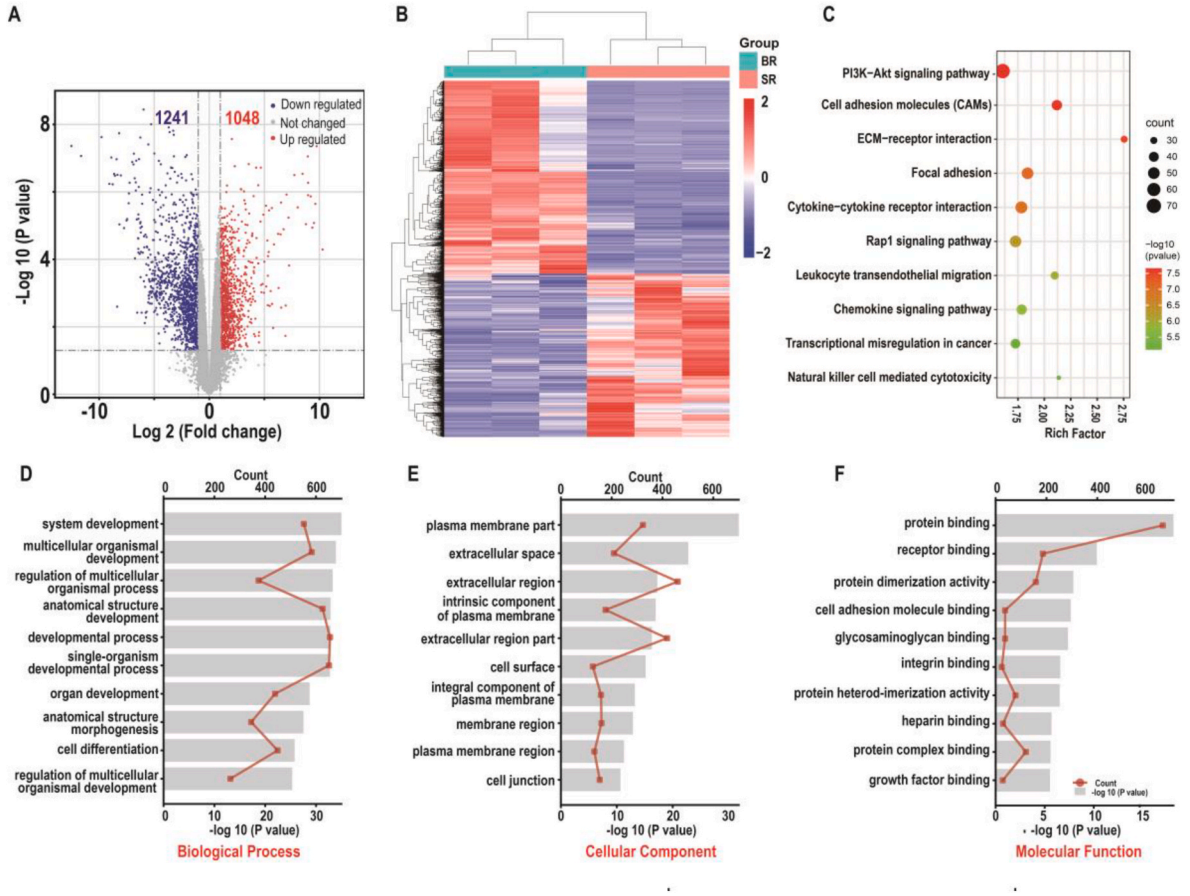

Fig. 3. Comparative transcriptomics of SCMECs and BMECs. (**A**) A volcano plot of RNA-seq results showing statistics of upregulated and downregulated genes (DEGs; $\log_2$ FC ≥ 1 or ≤ -1, respectively; *p-value* ≤ 0.05). (**B**) Heatmap of DEGs in SCMECs compared with BMECs. (**C**) A scatter plot of the top 10 KEGG pathways enriched among the DEGs. (**D**–**F**) Top 10 enriched GO biological processes (**D**), cellular components (**E**), and molecular functions (**F**). Red lines indicate the number of DEGs.

to immunity, such as complement and coagulation cascade (Fig. 4E). Notably, cell adhesion molecules pathway was the only pathway enriched among both DEGs and DEPs, which was involved in angiogenesis.

Combined transcriptomics and proteomics analysis revealed 82 differentially expressed genes and proteins (DEGPs) in the SCMECs group (FC ≥ 2 or ≤ -2 in both genes and proteins, *p-value* ≤ 0.05; Fig. 4F). Consistent with transcriptomics and proteomics results, KEGG enrichment analysis revealed that among the top 10 pathways, 6 were associated with immunity and metabolism (Fig. 4G). Furthermore, axon guidance and PPAR signaling pathways, which are associated with neuronal and NSC fate [49], were enriched in the top 10 DEGPs (Fig. 4G and Fig. S9). These results might suggest close associations between MECs and NSCs in the CNS.

3.4. SCMECs and BMECs display different angiogenic activities

As SCMECs and BMECs play crucial roles in the formation of BSCB and BBB and the neurovascular microenvironment of the CNS, we further compared their angiogenic activity. Analysis of angiogenesis-related gene expression [50] revealed differences between SCMECs and BMECs (Fig. 5A), especially in the mRNA levels of pro-angiogenic genes such as *Fgf1*, *Angtp2*, *VegfA*, and *PdgfA*, which were higher in BMECs than in SCMECs. Moreover, the expression of mechanosensory-related genes in SCMECs such as *Piezol*, and *Trpv* [51] were also higher in BMECs (Fig. 5B), and RT-qPCR further confirmed the expression trend in BMECs versus SCMECs such as angiogenesis-related genes *Anpep, Tgfb3,* and mechanosensory-related genes *Itga5* (Fig. S10).

Our previous study found that the angiogenic phenotype of liver sinusoidal endothelial cells could be induced in response to polyethylene glycol (PEG) hydrogels only within a certain modulus range, suggesting that endothelial cell angiogenesis could be regulated by stiffness stimulation [52]. As the biomechanical properties of spinal cord and brain tissue are different [53], therefore we further investigated the differences of *in vitro* angiogenesis induction between SCMECs and BMECs on hydrogels of different elastic moduli. The modulus of the polyethylene glycol (PEG) hydrogel could be adjusted by the PEG diacrylate (PEGDA) contents [30]. Rheometer testing proved the elastic modulus of obtained hydrogels were ranged from 50 to 3500 Pa, the more the PEGDA content in the hydrogel, the higher the modulus (Fig. S11). After culturing on the PEG hydrogels for 12 h, both SCMECs and BMECs acquired an angiogenic phenotype in tailored modulus (Fig. 5C, D and Fig. S12). Modulus of 50–1650 Pa was used for SCMECs, and of 50–300 Pa for BMECs (Fig. S11, Fig. 5C and D), consistent with the greater softness of brain (4.8 kPa for cortex) compared to that of the spinal cord (10 kPa) [53]. Immunofluorescence staining showed that the protein expression level of angiogenesis-related marker tight junction protein 1 (also known as zonula occludens-1, ZO-1) was higher in SCMECs and BMECs cultured on 0.2% PEG hydrogel than in those grown on tissue culture plates (Fig. 5E), suggesting more efficient induction of the angiogenic phenotype on the hydrogel with low stiffness. Similar results were obtained for F-actin staining (Fig. 5F).

3.5. SCMECs promote SNSC proliferation, migration, and differentiation

Previous reports have identified the vital significance of NSC in SCI repair and their close association with endothelial cells [21,54,55]. However, whether SCMECs and BMECs differ in their influence on

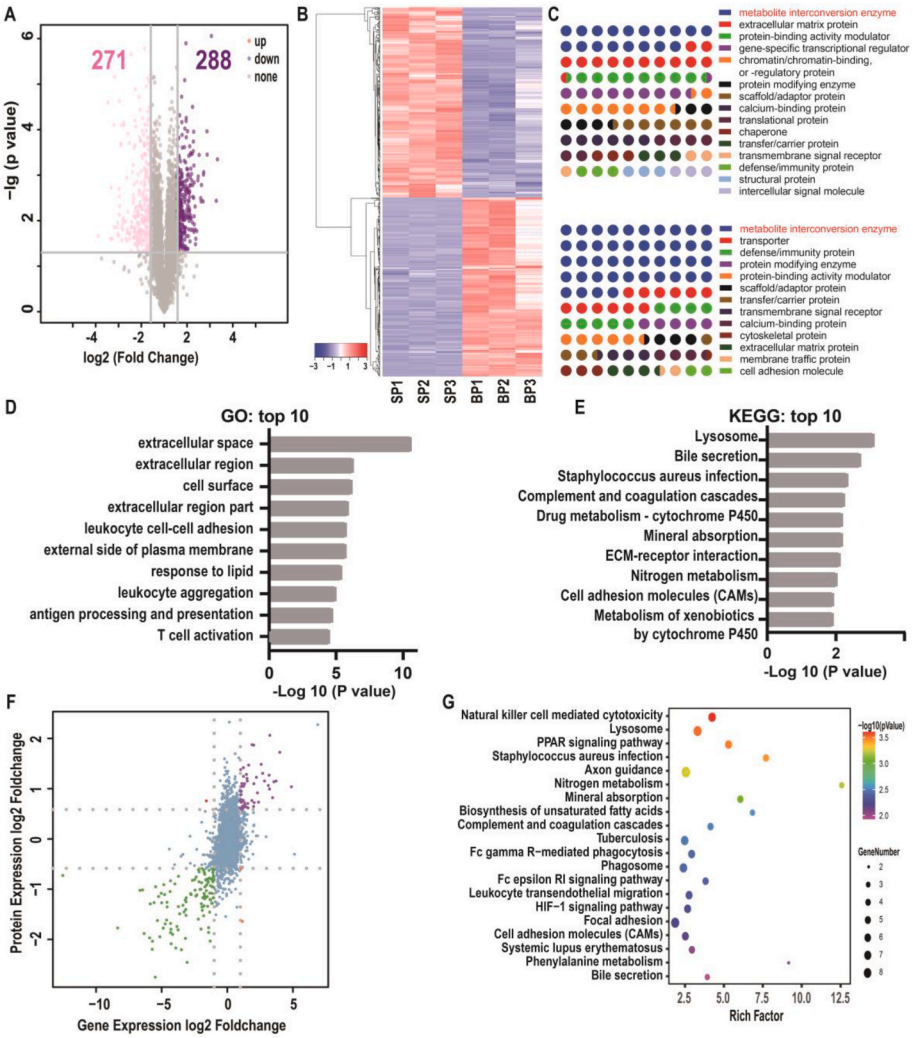

Fig. 4. Comparative proteomics and combined transcriptomics/proteomics of SCMECs and BMECs. (**A**) A volcano plot of differentially expressed proteins (DEPs) in SCMECs (FC $\geq$ 1.5 or $\leq$ 0.67 for upregulated (purple) or downregulated (pink) DEPS, respectively; *p-value* $\leq$ 0.05). (**B**) Proteomic clustering in SCMECs (SP1–3) compared to that in BMECs (BP1–3). (**C**) Classification of DEPs using the PANTHER system. (**D** and **E**) Top 10 enriched GO terms (**D**) and KEGG pathways (**E**) among the DEPs. (**F**) A volcano plot of differentially expressed genes and proteins (DEGPs) ($\log_2$ FC > 1 or < -1 for upregulated or downregulated DEGPs, respectively) identified by combined transcriptomics/proteomics analysis. (**G**) A scatter plot of top 20 enriched KEGG pathways among the DEGPs.

SNSCs and BNSCs remains unknown. To address this question, we co-cultured BNSCs and SNSCs with SCMECs or BMECs in transwell plates.

Typical BNSCs and SNSCs spheroids expressing NSC markers, nestin and Sox2, were obtained after 5–7 days of culture (Fig. S13). Moreover, the obtained cells demonstrated the ability to differentiate into neurons and glial cells, evidenced by the expression of neuron-specific class III beta-tubulin (Tuj1) and astrocyte-specific glial fibrillary acidic protein (GFAP), respectively (Fig. S13). Co-culture of BNSCs or SNSCs with BMECs or SCMECs showed that both types of endothelial cells induced the proliferation of BNSCs and SNSCs, evidenced by an increased number of EdU-positive cells (Fig. 6A and B). The effect of SCMECs on BNSCs was stronger than that of BMECs; however, there was no significant difference between the effect of both MECs in SNSCs (Fig. 6A and B).

The effect of MECs on NSC migration was analyzed by seeding the SNSC or BNSC neurospheres on the poly-D-lysine (PDL)-coated lower compartment of plates, and co-culturing them with or without BMECs or SCMECs for 24 h (Fig. 6C). The migration distances of SNSCs were longer than those of BNSCs in non-conditional medium (Fig. 6D and E), suggesting that SNSCs had a higher ability to migrate than BNSCs. Both SCMECs and BMECs positively affected BNSC and SNSC migration; however, the effect of BMECs was more pronounced (Fig. 6D and E). Similar results were obtained using conditioned medium (CM) from BMEC or SCMEC cultures. Both CM stimulated NSC migration; however, a dose-response effect was observed only with BMEC-CM (Fig. 6F and G), confirming that the stronger effect of BMECs on BNSC/SNSC migration.

Finally, we tested the influence of BMECs and SCMECs on NSC differentiation. Co-culture of BNSCs with BMECs or SCMECs increased the number of Tuj1-positive cells and decreased the number of GFAP-positive cells, compared to BNSC control conditions (Fig. 6H and I). Similarly, co-culture of SNSCs with BMECs or SCMECs increased the number of Tuj1-positive cells (Fig. 6H and I). These results indicated that both BMECs and SCMECs stimulate NSC differentiation, in agreement with previous reports on the beneficial effect of endothelial cells on NSC differentiation [21,56].

3.6. SCMEC transplantation promotes vascular reconstruction

Considering the crucial roles of SCMECs in the spinal cord microenvironment and their positive effects on NSC proliferation, migration, and differentiation, we hypothesized that they could exhibit positive effects on SCI repair. To test this hypothesis, we explored the therapeutic effect of SCMECs and BMECs in combination with NeuroRegen using an in vivo model of complete SCI (Fig. 7A and Fig. S14). Different numbers of GFP-labeled SCMECs or BMECs (0.25×10^6, 1×10^6, or 4×10^6; groups designated as SC./BC., SC1/BC1, or SC4/BC4, respectively) were seeded on NeuroRegen scaffolds overnight, and the compatibility of NeuroRegen for transplanted cells was confirmed using live/dead cell staining and scanning electron microscopy (SEM). Cells cultured on NeuroRegen showed spreading morphologies by F-actin staining and

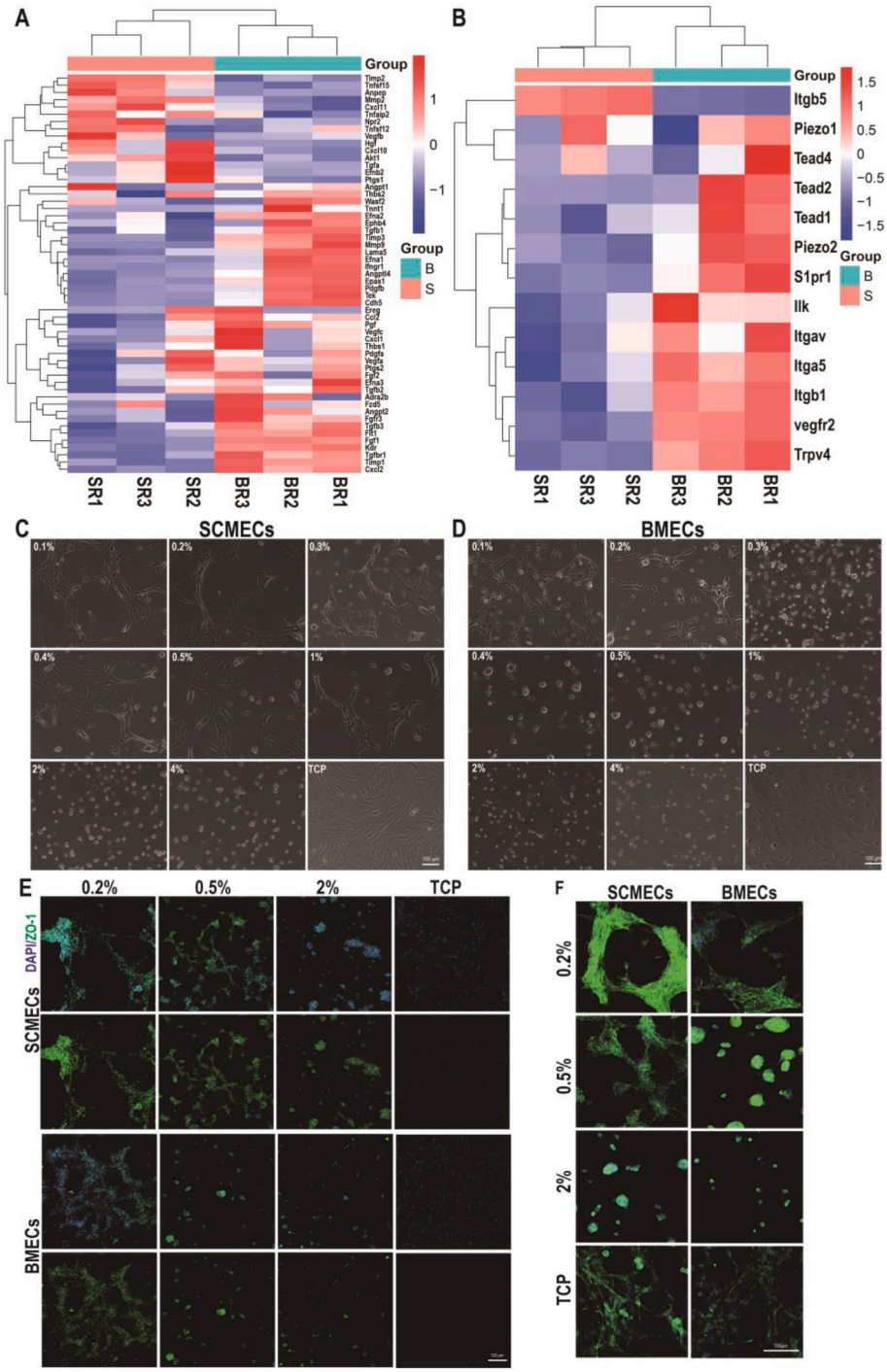

Fig. 5. Comparison of angiogenesis in SCMECs and BMECs. (**A**) Heatmap of angiogenesis-related genes. (**B**) Heatmap of mechanical sensors-related genes. (**C** and **D**) Morphology of SCMECs (**C**) and BMECs (**D**) cultured on PEG hydrogels with different PEGDA content and elastic modulus. Scale bar, 100 μm. (**E** and **F**) Representative immunofluorescence images of SCMECs and BMECs (**F**) cultured on PEG hydrogels prepared with different PEGDA concentrations. Cells were stained with DAPI (blue) and antibodies against ZO-1 (green; **E**) and F-actin (green; **F**); scale bar, 100 μm.

improved proliferation ratio tested by alamarBlue staining (Fig. S15). Cells were then transplanted into rats with complete SCI for 10 days (early-stage; Fig. S16) or 8 weeks (late-stage), and the number of GFP-labeled SMECs/BMECs remained in the injured spinal cord tissue was positively correlated with the initial number of transplanted cells (Fig. S17).

Then, we further examined the neovascularization at the lesion site in early-stage and late-stage SCI repair. Treatment with SCMECs or BMECs in combination with NeuroRegen increased the blood vessel density at early-stage SCI, compared to that in the Scaffold or Sci groups. As evidenced by the expression of endothelial cell antigen RECA-1, SCMECs-treated rats exhibited more blood vessels at the SCI site than BMEC-treated rats; moreover, the largest number of microvessels was observed in the SC1 group rather than in the SC4 group (Fig. 7D, E, and H), indicating that 1×10^6 SCMECs integrated into NeuroRegen was the most effective combination for vascular reconstruction at early-stage SCI. Similarly, the SC1 group showed a significantly higher degree of neovascularization than the BC1 and scaffold groups at late-stage SCI (Fig. 7F, G, and I). Also, immunofluorescent staining results showed that ZO-1 expression level in the SC1 group was the highest among all the groups, possibly suggesting enhanced neovascularization after SCMECs transplantation (Fig. S18). *In vitro* RNA-seq data showed that 17 genes related with angiogenesis regulation were expressed 10 or more times higher in SCMECs than in BMECs (Fig. 7J), which might be benefit for neovascularization after implantation. Moreover, the higher expression levels of *Gata4, Hcar1, Mepe, Il17b* and *Esm1* in SCMECs were related

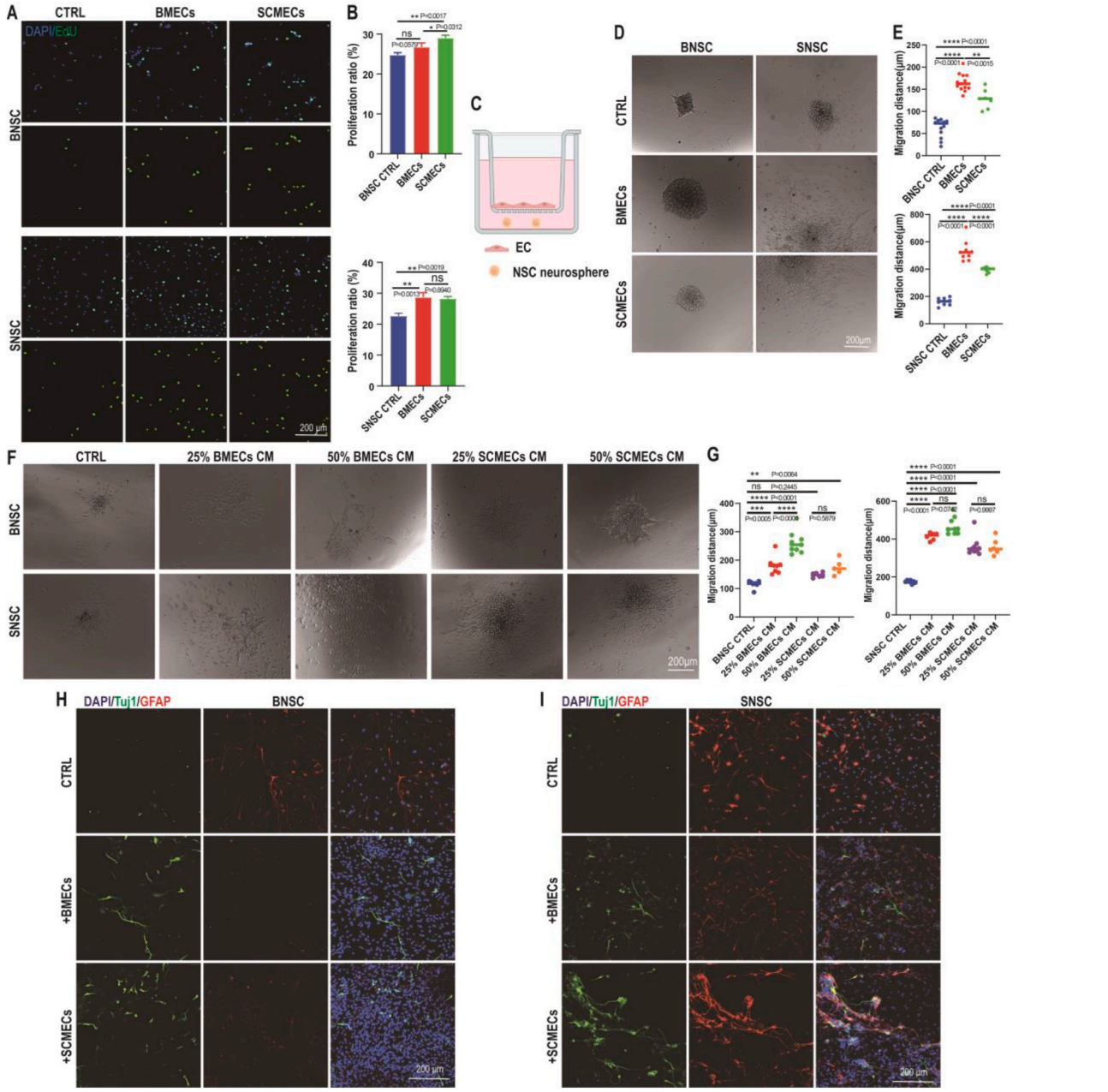

Fig. 6. Effects of SCMECs and BMECs on BNSCs and SNSCs. (**A**) Representative immunofluorescence images of BNSCs and SNSCs stained with EdU (green) and DAPI (blue). Scale bar, 200 μm. (**B**) The proliferation ratio (EdU-positive/DAPI-positive) of BNSCs (upper graph) and SNSCs (lower graph) in the presence of SCMECs and BMECs (n = 3 per group); $*p < 0.05$ and $**p < 0.01$ using the *one-way ANOVA*. (**C**–**E**) Effect of MECs on NSC migration. Schematic representation of the transwell system used in the test: NSC neurospheres were placed on the bottom of a PDL-coated plate and ECs were placed in the insert (**C**). Representative Images of BNSCs and SNSCs cultured with SCMECs and BMECs are shown (CTRL, control) (**D**). Graphs present the migration distance of BNSCs (upper) and SNSCs (lower) cultured with SCMECs or BMECs (n > 7 per group); $***p = 0.0001$ and $****p < 0.0001$ (**E**). (**F** and **G**) Effects of SCMEC and BMEC conditioned medium (CM) on NSC migration. Images of migrated BNSCs and SNSCs cultured with the indicated CM concentrations (**F**). Quantitative analysis of NSC migration distance (n > 6 per group); $*p < 0.05$, $**p < 0.01$, $***p = 0.0001$, and $****p < 0.0001$ (**G**). (**H** and **I**) Effect of SCMECs and BMECs on BNSC (**H**) and SNSC (**H**) differentiation analyzed using immunofluorescence. Tuj1, green; GFAP, red; DAPI, blue. Scale bar, 200 μm.

with VEGF secretion [57]. Hence, it's assumed that VEGF-PI3K-AKT signaling pathway might involve SCMECs vascular reconstruction in SCI rats. Immunohistochemistry and western blot analysis found that higher expression levels of VEGF, AKT, and phosphor-endothelial nitric-oxide synthase (eNOS) in the SC1 group than BC1 group at 8 weeks post-treatment in SCI (Fig. 7K and L).

Endothelial cells also play an important role in regulating inflammatory responses, which were evaluated after MECs transplantation through the expression of reactive microglia/macrophage marker, CD68. Highest CD68 expression levels were observed in the BC4 group and rather high in the SC4 group, but the lowest in the SC1 group (Fig. 8A and B and Fig. S19), suggesting that inflammation could be responsible for the weaker vascularization of SC4/BC4 in SCI repair. The expression levels of a M2 macrophage marker, CD206, were also characterized at early stage (Fig. S19). More CD206+ cells were observed in the SC1 group, indicating higher level of anti-inflammatory effects of a certain concentration of SCMECs, which might lead to better therapeutic effects [58–60].

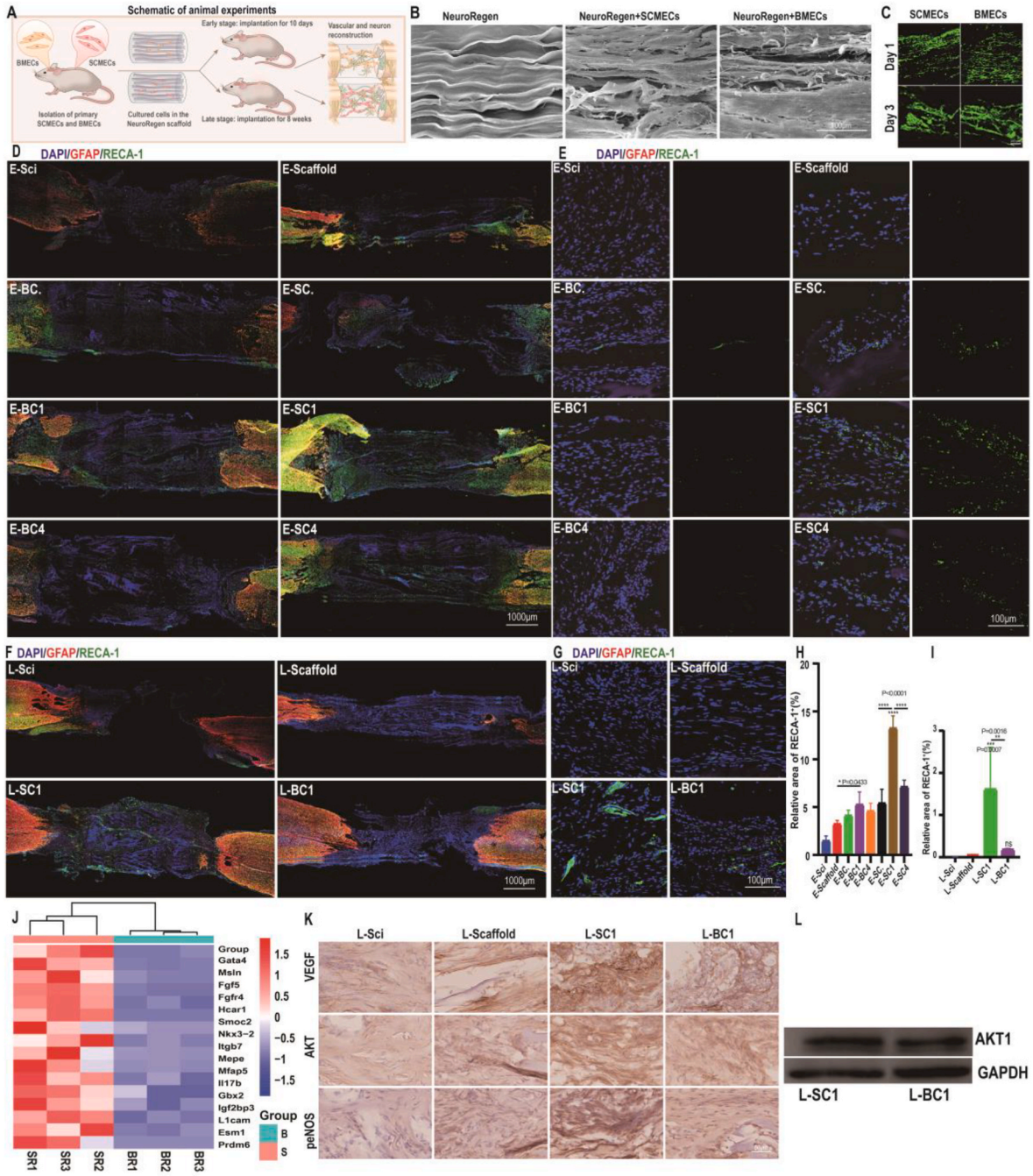

Fig. 7. Transplanted SMECs/BMECs affect vascular reconstruction after SCI. (**A**) Schematic representation of the experimental design. SCMECs or BMECs loaded on NeuroRegen scaffolds were transplanted into the lesion site of rats with complete SCI. (**B**) Representative SEM images of SCMECs or BMECs cultured on NeuroRegen for 2 days. Scale bar, 100 μm. (**C**) Live-dead staining of SCMECs and BMECs cultured on NeuroRegen for 1 day and 3 days. Scale bar, 200 μm. (**D** and **E**) RECA-1 immunostaining of the spinal cord at early-stage SCI; scale bars, 1000 μm (**D**) and 100 μm (SCI zone, **E**). GFAP, red; RECA-1, green; DAPI, blue. (**F** and **G**) RECA-1 immunostaining of the spinal cord at late-stage SCI; scale bars, 1000 μm (**F**) and 100 μm (SCI zone, **G**). GFAP, red; RECA-1, pink; DAPI, blue. (**H** and **I**) Quantification of RECA-1-positive blood vessels in the early-stage (H) and late-stage SCI zone (I). (**J**) RNA sequencing results of the expression of genes related to angiogenesis regulation of. (**K** and **L**) Immunohistochemistry (**K**) and western blot analysis (**L**) of proteins in the VEGF-PI3K/AKT/eNOS signaling pathway.

3.7. SCMECs stimulate neuronal regeneration and functional recovery in SCI rats

Migration and neural differentiation of endogenous NSCs were thought to be essential for the replacement of lost neural cells at the injured site. Immunostaining of the injured spinal cord for nestin in early-stage SCI revealed that the number of NSCs was increased after transplantation of SCMECs or BMECs compared to that of NeuroRegen alone, being the highest in the SC1 group (Fig. 8C, D, and Fig. S20). However, no significant difference were found between the SC1 and BC1 groups, suggesting that both SCMECs and BMECs could recruit endogenous NSCs into the lesion site at early-stage SCI. Furthermore, Tuj1-positive cell number was higher in rats treated with SCMECs or BMECs than in those treated with the scaffold alone; the highest numbers were detected in the SC1 and BC1 groups (Fig. 8E and F). More Tuj1-positive neurons at the lesion site and more mature neuronal cells (positive for microtubule-associated protein 2 [MAP2], serotonin [5-HT], and choline acetyltransferase [ChAT]) in the SC1 group at late-

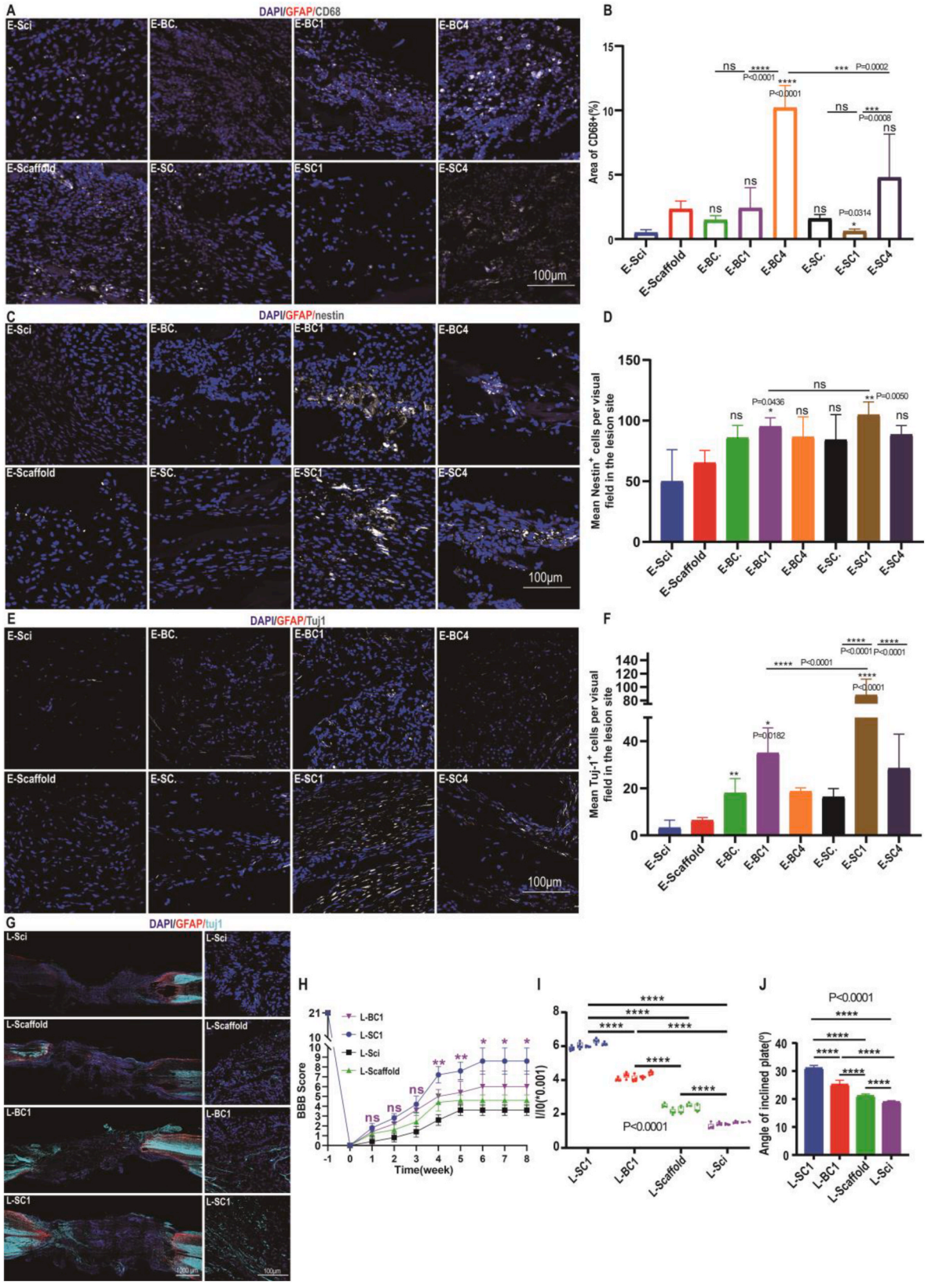

Fig. 8. Transplanted SCMECs promoted neural niches and motor function recovery in rats with SCI. (**A** and **B**) Representative images of CD68-positive areas (**A**) and quantitative analysis (**B**) for early-stage SCI. GFAP red; CD68, gray; DAPI, blue. Scale bar, 100 μm. (**C** and **D**) Representative images of nestin-positive areas (**C**) and quantitative analysis (**D**) for early-stage SCI. GFAP, red; nestin, gray; DAPI, blue. Scale bar, 100 μm. (**E** and **F**) Representative images of Tuj1-positive areas (**E**) and quantitative analysis (**F**) for early-stage SCI. GFAP, red; Tuj1, gray; DAPI, blue. Scale bar, 100 μm. (**G**) Representative images of Tuj1-positive areas for late-stage SCI. Scale bars, 1000 μm (left) or 100 μm (lesion site, right). GFAP, red; Tuj1, cyan; DAPI, blue. **(H)** Hindlimb Basso-Beattie-Bresnahan scores. **(I)** Relative corresponding signals of hindlimb strengths were recorded by the pressure sensorat 8 weeks post-SCI. **(J)** Inclined plane assay results at 8 weeks post-SCI for the indicated animal groups (n = 3 per group).

stage treatment than those in the BC1 and scaffold groups (Fig. 8G, and Fig. S21). Moreover, luxol fast blue (LFB) staining revealed increased myelin deposition in the SC1 group (Fig. S22). Overall, these findings indicated that transplanted SCMECs at certain dose were more effective than BMECs in promoting neuronal regeneration at both early- and late-stage SCI.

Finally, we analyzed motor function restoration in SCI rats after treatment with SC1 and BC1 preparations, using the Basso, Beattie, and Bresnahan locomotor rating scale. The SC1 and BC1 groups exhibited significantly higher scores (8.0 and 6.0, respectively) than the Sci group at week 6 (Fig. 8H). Furthermore, SC1 and BC1 administration significantly increased hindlimb strength at week 8 post-transplantation, which was higher in the SC1 group (Fig. 8I). The inclined plane test revealed wider angles in the SC1 (31°) and BC1 (25°) groups than in the Sci group (19°; Fig. 8J). These data indicate that the transplantation of MECs promotes motor function recovery after SCI and that the therapeutic effect of SCMECs is significantly stronger than that of BMECs.

4. Discussion

Endothelial cells are considered key factors for SCI repair owing to their role in vascular reestablishment, producing a microenvironment conducive to neuronal regeneration, thus playing crucial roles in spinal cord homeostasis, pathogenesis, and reconstruction. In embryonic and adult stages [61], a phenomenon called neurovascular congruence showing functionally and physically interdependent in the vascular and nervous systems is widespread, suggesting close association of vascular system with neural microenvironment. Moreover, it was reported that endothelial cells direct axon growth in SCI model and improve neurogenesis; In the brain, BMECs were found to regulate NSC differentiation fate by secreting bioactive factors [62] and provide *trans*-differentiation signals to reprogram astrocytes into NSC [63]. In addition, influence of endothelial cells on NSC have been reported [21,56,64], and the proliferation and differentiation of neural progenitor cells is accompanied by vascularization of the central nervous system to meet the increasing demand for nutrients and oxygen, suggesting a close relationship between neovascularization and neurogenesis [65]. Furthermore, in the adult SCI rats, axonal regeneration was found to be regulated by neovascularization secretion factors and distributed in the direction of neovascularization [23]. Konstantinos et al. summarized many kinds of angiogenesis administrators for spinal cord treatment, showing close correlation between angiogenesis and functional recovery after SCI [66]. Considering the dual positive effects of endothelial cells including MECs on modulation neural regeneration and vascular microenvironment reestablishment, human umbilical vein endothelial cells transplantation further implied functional recovery in SCI repair [67,68], suggesting CNS-derived endothelial cells including MECs may be great potential candidates to promote SCI repair.

However, to the best of our knowledge, there are no reports yet of the use of SCMECs or BMECs for spinal cord regeneration after SCI. Our present findings indicate that at certain dose, SCMECs promote vascular reconstruction, neuronal regeneration, and functional improvement in rats with SCI more effectively than BMECs. Similar results were observed in our previous studies revealing more effectiveness of SNSCs than NSCs from other sources in SCI repair [24,69], suggesting that tissue-specific origin of cells used for transplantation is a factor to be considered in SCI repair, and more potent of SCMECs in stimulating SCI functional recovery than BMECs.

It was observed there was no significant difference in the number of endogenous SNSCs at the injury site after transplantation of the same number of SCMECs and BMECs in the SCI and BC1 groups. This appears to contradict the stronger effect of BMECs on SCNSC migration; however, this phenomenon could be explained by the higher vascular reconstruction at the injury site in the SC1 group compared to that in the BC1 group, which improved the effects of SCMECs on SCNSC migration. The higher levels of vascular reestablishment may further enhance the SCMECs therapeutic effects on SCI repair.

It was SC1 group, not SC4 group showed a better therapeutic effect in SCI repair, which seemed the effects of transplanted SCMECs or BMECs on angiogenesis or neurogenesis did not present a dose-dependent manner. This was probable due to the higher levels of immune responses (Fig. 8A and B) induced by the excessive exogenous cell transplantation. Besides, Maciej et al. analyzed MSC dose-response in clinical trials to reveal that MSC treatment in clinical trials was ineffective if the dosage was too low or high [70], suggesting only an appropriate number of implanted cells can obtain better therapeutic effects in treatment of diseases.

Transcriptomic and proteomic profiling revealed inherent differences between SCMECs and BMECs were mainly focused on metabolism-, immunity-, and angiogenesis-related signaling pathways. These results are consistent with the notion that endothelial cells participate in immune responses [71,72], strengthening the hypothesis that MECs play a crucial role in the immune microenvironment of the CNS and further in-depth studies are needed. In addition, the Rap1 pathway involved in the endothelial barrier function was also enriched in our transcriptomic analysis, consistent with the reported differences between BSCB and BBB [18]. The PI3K-AKT signaling pathway, which ranked first in the KEGG analysis of DEGs in our results, has been reported closely associated with angiogenesis and performed an essential role in the pathological process of SCI [73,74]. For instance, insulin-like growth factor-1-induced PI3K-AKT signaling activation reduced MEC apoptosis and microvascular damage after SCI. And activating PI3K-AKT signaling pathway by inhibiting phosphatase and tensin homolog promoted axon growth and recovery of locomotor function in SCI mouse model [75]. These investigations highlighted the importance of the PI3K-AKT signaling pathway in vascular and neural microenvironment in SCI. Additionally, we also found that higher levels of VEGF, AKT, and eNOS were detected in the SCI rats with SCMEC treatment, which is consist with the results of SCMEC characteristics, and might contribute to the higher SCI repair efficiency of SCMECs.

5. Conclusion

In this study, we established an efficient protocol for SCMEC and BMEC isolation from adult rats. Furthermore, we uncovered differences between SCMECs and BMECs in angiogenesis-related genes, proteins, signaling pathways and responsibility to stiffness stimulation. Using complete SCI rat model, we found that the transplantation of certain dose SCMECs loaded on the NeuroRegen scaffold showed superior results than that of BMECs in vascular reconstruction and inflammatory regulation, consequently improving neural regeneration. We also highlight the VEGF/AKT/eNOS- mediated signaling pathway as a potential underlying mechanism of this phenomenon involved in SCMEC-promoted neovascularization and neuronal regeneration. Our study will facilitate clinical translational research of SCMECs in terms of therapeutic application.

Ethics approval

All animal experiments were approved by the Institutional Animal Care and Use Committee and conducted following the governmental and the Chinese Academy of Sciences guidelines for animal welfare (approval NO. SINANO/EC/2021-026).

Author contributions

Z.Y., H.S., and J.D. conceived and designed the experiments; Z.Y. designed and established primary SCMECs and BMECs isolation system; Z.Y. and X.G. designed and performed in vivo experiments and data processing with help from W.Y.; T. X., X.K., Y.Z. and W.Y helped to characterize PEG hydrogel; X.K. did western blotting test; X.G., Y.L., and T.Z. helped in testing hindlimb strengths; F.W. helped in SEM analysis;

Y.S. provided technical support; Z.Y. and X.G. wrote the manuscript, which H.S. and J.D. helped to revise.

Declaration of competing interest

The authors declare no competing interests.

Acknowledgments

This work was supported by grants from the National Natural Science Foundation of China (Nos. 81891002, 81971178, 32200806), the Strategic Priority Research Program of the Chinese Academy of Sciences (No. XDA16040701), the Youth Innovation Promotion Association CAS (No. 2021319), the Natural Science Foundation of Jiangsu Province (No. BK20210127), and the High-level Innovation and Entrepreneurship Talent Introduction Plan of Jiangsu Province.

We acknowledge the CapitalBio Technology Inc. (Beijing, China) for RNA sequencing and proteomic sequencing. Schematic in Fig. 2A and 6C were created with BioRender.com and were granted publication permission. We acknowledge a kind gift of PEGDA from Prof. Y. Du (Tsinghua University, Beijing, China) and help from PhD candiate WJ. Li in his lab on schematic preparation.

Appendix A. Supplementary data

Supplementary data to this article can be found online at https://doi.org/10.1016/j.bioactmat.2023.06.019.

References

[1] A.F. Cristante, T.E. Barros Filho, R.M. Marcon, O.B. Letaif, I.D. Rocha, Therapeutic approaches for spinal cord injury, Clinics 67 (10) (2012) 1219–1224, https://doi.org/10.6061/clinics/2012(10)16.

[2] G.B.D.T.B. Injury, C. Spinal Cord Injury, Global, regional, and national burden of traumatic brain injury and spinal cord injury, 1990-2016: a systematic analysis for the global burden of disease study 2016, Lancet Neurol. 18 (1) (2019) 56–87, https://doi.org/10.1016/S1474-4422(18)30415-0.

[3] A. Alizadeh, S.M. Dyck, S. Karimi-Abdolrezaee, Traumatic spinal cord injury: an overview of pathophysiology, models and acute injury mechanisms, Front. Neurol. 10 (2019) 282, https://doi.org/10.3389/fneur.2019.00282.

[4] H. Shen, C. Fan, Z. You, Z. Xiao, Y. Zhao, J. Dai, Advances in biomaterial-based spinal cord injury repair, Adv. Funct. Mater. 32 (13) (2022), 2110628, https://doi.org/10.1002/adfm.202110628.

[5] Y. Zhang, A. Al Mamun, Y. Yuan, Q. Lu, J. Xiong, S. Yang, C. Wu, Y. Wu, J. Wang, Acute spinal cord injury: pathophysiology and pharmacological intervention (review), Mol. Med. Rep. 23 (6) (2021) 1–18, https://doi.org/10.3892/mmr.2021.12056.

[6] D.M. Cohen, C.B. Patel, P. Ahobila-Vajjula, L.M. Sundberg, T. Chacko, S.J. Liu, P. A. Narayana, Blood-spinal cord barrier permeability in experimental spinal cord injury: dynamic contrast-enhanced mri, NMR Biomed. 22 (3) (2009) 332–341, https://doi.org/10.1002/nbm.1343.

[7] J.T. Maikos, D.I. Shreiber, Immediate damage to the blood-spinal cord barrier due to mechanical trauma, J. Neurotrauma 24 (3) (2007) 492–507, https://doi.org/10.1089/neu.2006.0149.

[8] W.D. Whetstone, J.Y. Hsu, M. Eisenberg, Z. Werb, L.J. Noble-Haeusslein, Blood-spinal cord barrier after spinal cord injury: relation to revascularization and wound healing, J. Neurosci. Res. 74 (2) (2003) 227–239, https://doi.org/10.1002/jnr.10759.

[9] S. Yu, S. Yao, Y. Wen, Y. Wang, H. Wang, Q. Xu, Angiogenic microspheres promote neural regeneration and motor function recovery after spinal cord injury in rats, Sci. Rep. 6 (2016), 33428, https://doi.org/10.1038/srep33428.

[10] H. Kumar, M.J. Jo, H. Choi, M.S. Muttigi, S. Shon, B.J. Kim, S.H. Lee, I.B. Han, Matrix metalloproteinase-8 inhibition prevents disruption of blood-spinal cord barrier and attenuates inflammation in rat model of spinal cord injury, Mol. Neurobiol. 55 (3) (2018) 2577–2590, https://doi.org/10.1007/s12035-017-0509-3.

[11] J. Kawabe, M. Koda, M. Hashimoto, T. Fujiyoshi, T. Furuya, T. Endo, A. Okawa, M. Yamazaki, Neuroprotective effects of granulocyte colony-stimulating factor and relationship to promotion of angiogenesis after spinal cord injury in rats: laboratory investigation, J. Neurosurg. Spine 15 (4) (2011) 414–421, https://doi.org/10.3171/2011.5.SPINE10421.

[12] H. Kumar, C.S. Lim, H. Choi, H.P. Joshi, K.T. Kim, Y.H. Kim, C.K. Park, H.M. Kim, I. B. Han, Elevated trpv4 levels contribute to endothelial damage and scarring in experimental spinal cord injury, J. Neurosci. 40 (9) (2020) 1943–1955, https://doi.org/10.1523/JNEUROSCI.2035-19.2020.

[13] S. Ni, Z. Luo, L. Jiang, Z. Guo, P. Li, X. Xu, Y. Cao, C. Duan, T. Wu, C. Li, H. Lu, J. Hu, Utx/kdm6a deletion promotes recovery of spinal cord injury by epigenetically regulating vascular regeneration, Mol. Ther. 27 (12) (2019) 2134–2146, https://doi.org/10.1016/j.ymthe.2019.08.009.

[14] P. Assinck, G.J. Duncan, B.J. Hilton, J.R. Plemel, W. Tetzlaff, Cell transplantation therapy for spinal cord injury, Nat. Neurosci. 20 (5) (2017) 637–647, https://doi.org/10.1038/nn.4541.

[15] J. Zhong, J. Xu, S. Lu, Z. Wang, Y. Zheng, Q. Tang, J. Zhu, T. Zhu, A prevascularization strategy using novel fibrous porous silk scaffolds for tissue regeneration in mice with spinal cord injury, Stem Cell. Dev. 29 (9) (2020) 615–624, https://doi.org/10.1089/scd.2019.0199.

[16] S. Nori, Y. Okada, A. Yasuda, O. Tsuji, Y. Takahashi, Y. Kobayashi, K. Fujiyoshi, M. Koike, Y. Uchiyama, E. Ikeda, Y. Toyama, S. Yamanaka, M. Nakamura, H. Okano, Grafted human-induced pluripotent stem-cell-derived neurospheres promote motor functional recovery after spinal cord injury in mice, Proc. Natl. Acad. Sci. U. S. A. 108 (40) (2011) 16825–16830, https://doi.org/10.1073/pnas.1108077108.

[17] L.Y. Jin, J. Li, K.F. Wang, W.W. Xia, Z.Q. Zhu, C.R. Wang, X.F. Li, H.Y. Liu, Blood-spinal cord barrier in spinal cord injury: a review, J. Neurotrauma 38 (9) (2021) 1203–1224, https://doi.org/10.1089/neu.2020.7413.

[18] V. Bartanusz, D. Jezova, B. Alajajian, M. Digicaylioglu, The blood-spinal cord barrier: Morphology and clinical implications, Ann. Neurol. 70 (2) (2011) 194–206, https://doi.org/10.1002/ana.22421.

[19] J.M. Fassbender, S.R. Whittemore, T. Hagg, Targeting microvasculature for neuroprotection after sci, Neurotherapeutics 8 (2) (2011) 240–251, https://doi.org/10.1007/s13311-011-0029-1.

[20] S. Puentes, M. Kurachi, K. Shibasaki, M. Naruse, Y. Yoshimoto, M. Mikuni, H. Imai, Y. Ishizaki, Brain microvascular endothelial cell transplantation ameliorates ischemic white matter damage, Brain Res. 1469 (2012) 43–53, https://doi.org/10.1016/j.brainres.2012.06.042.

[21] Q. Shen, S.K. Goderie, L. Jin, N. Karanth, Y. Sun, N. Abramova, P. Vincent, K. Pumiglia, S. Temple, Endothelial cells stimulate self-renewal and expand neurogenesis of neural stem cells, Science 304 (5675) (2004) 1338–1340, https://doi.org/10.1126/science.1095505.

[22] Q.J. Yu, H. Tao, X. Wang, M.C. Li, Targeting brain microvascular endothelial cells: a therapeutic approach to neuroprotection against stroke, Neural Regen Res 10 (11) (2015) 1882–1891, https://doi.org/10.4103/1673-5374.170324.

[23] P.P. Partyka, Y. Jin, J. Bouyer, A. DaSilva, G.A. Godsey, R.G. Nagele, I. Fischer, P. A. Galie, Harnessing neurovascular interaction to guide axon growth, Sci. Rep. 9 (1) (2019) 2190, https://doi.org/10.1038/s41598-019-38558-y.

[24] Y. Zou, D. Ma, H. Shen, Y. Zhao, B. Xu, Y. Fan, Z. Sun, B. Chen, W. Xue, Y. Shi, Z. Xiao, R. Gu, J. Dai, Aligned collagen scaffold combination with human spinal cord-derived neural stem cells to improve spinal cord injury repair, Biomater. Sci. 8 (18) (2020) 5145–5156, https://doi.org/10.1039/d0bm00431f.

[25] Y. Zhu, B. Kong, R. Liu, Y. Zhao, Developing biomedical engineering technologies for reproductive medicine, Smart Medicine 1 (1) (2022), e20220006, https://doi.org/10.1002/SMMD.20220006.

[26] W. Xue, W. Shi, Y. Kong, M. Kuss, B. Duan, Anisotropic scaffolds for peripheral nerve and spinal cord regeneration, Bioact. Mater. 6 (11) (2021) 4141–4160, https://doi.org/10.1016/j.bioactmat.2021.04.019.

[27] Y. Zhao, F. Tang, Z. Xiao, G. Han, N. Wang, N. Yin, B. Chen, X. Jiang, C. Yun, W. Han, C. Zhao, S. Cheng, S. Zhang, J. Dai, Clinical study of neuroregen scaffold combined with human mesenchymal stem cells for the repair of chronic complete spinal cord injury, Cell Transplant. 26 (5) (2017) 891–900, https://doi.org/10.3727/096368917X695038.

[28] Z. Xiao, F. Tang, J. Tang, H. Yang, Y. Zhao, B. Chen, S. Han, N. Wang, X. Li, S. Cheng, G. Han, C. Zhao, X. Yang, Y. Chen, Q. Shi, S. Hou, S. Zhang, J. Dai, One-year clinical study of neuroregen scaffold implantation following scar resection in complete chronic spinal cord injury patients, Sci. China Life Sci. 59 (7) (2016) 647–655, https://doi.org/10.1007/s11427-016-5080-z.

[29] Y. Yang, Y. Fan, H. Zhang, Q. Zhang, Y. Zhao, Z. Xiao, W. Liu, B. Chen, L. Gao, Z. Sun, X. Xue, M. Shu, J. Dai, Small molecules combined with collagen hydrogel direct neurogenesis and migration of neural stem cells after spinal cord injury, Biomaterials 269 (2021), 120479, https://doi.org/10.1016/j.biomaterials.2020.120479.

[30] X. Fan, L. Zhu, K. Wang, B. Wang, Y. Wu, W. Xie, C. Huang, B.P. Chan, Y. Du, Stiffness-controlled thermoresponsive hydrogels for cell harvesting with sustained mechanical memory, Adv Healthc Mater 6 (5) (2017), 1601152, https://doi.org/10.1002/adhm.

[31] Z. Luo, J. Che, L. Sun, L. Yang, Y. Zu, H. Wang, Y. Zhao, Microfluidic electrospray photo-crosslinkable κ-carrageenan microparticles for wound healing, Engineered Regeneration 2 (2021) 257–262, https://doi.org/10.1016/j.engreg.2021.10.002.

[32] H. Lin, B. Chen, B. Wang, Y. Zhao, W. Sun, J. Dai, Novel nerve guidance material prepared from bovine aponeurosis, J. Biomed. Mater. Res. 79 (3) (2006) 591–598, https://doi.org/10.1002/jbm.a.30862.

[33] D.M. Basso, M.S. Beattie, J.C. Bresnahan, Graded histological and locomotor outcomes after spinal cord contusion using the nyu weight-drop device versus transection, Exp. Neurol. 139 (2) (1996) 244–256, https://doi.org/10.1006/exnr.1996.0098.

[34] X. Gao, Z. You, Y. Li, X. Kang, W. Yang, H. Wang, T. Zhang, X. Zhao, Y. Sun, H. Shen, J. Dai, Multifunctional hydrogel modulates the immune microenvironment to improve allogeneic spinal cord tissue survival for complete spinal cord injury repair, Acta Biomater. 155 (2023) 235–246, https://doi.org/10.1016/j.actbio.2022.11.015.

[35] A.S. Rivlin, C.H. Tator, Objective clinical assessment of motor function after experimental spinal cord injury in the rat, J. Neurosurg. 47 (4) (1977) 577–581, https://doi.org/10.3171/jns.1977.47.4.0577.

[36] S. Han, Z. Xiao, X. Li, H. Zhao, B. Wang, Z. Qiu, Z. Li, X. Mei, B. Xu, C. Fan, B. Chen, J. Han, Y. Gu, H. Yang, Q. Shi, J. Dai, Human placenta-derived mesenchymal stem cells loaded on linear ordered collagen scaffold improves functional recovery after completely transected spinal cord injury in canine, Sci. China Life Sci. 61 (1) (2018) 2–13, https://doi.org/10.1007/s11427-016-9002-6.
[37] X. Meng, B. Grotsch, Y. Luo, K.X. Knaup, M.S. Wiesener, X.X. Chen, J. Jantsch, S. Fillatreau, G. Schett, A. Bozec, Hypoxia-inducible factor-1alpha is a critical transcription factor for il-10-producing b cells in autoimmune disease, Nat. Commun. 9 (1) (2018) 251, https://doi.org/10.1038/s41467-017-02683-x.
[38] P.M.D. Watson, J.C. Paterson, G. Thom, U. Ginman, S. Lundquist, C.I. Webster, Modelling the endothelial blood-cns barriers: a method for the production of robust in vitromodels of the rat blood-brain barrier and blood-spinal cord barrier, BMC Neurosci. 14 (1) (2013) 59, https://doi.org/10.1186/1471-2202-14-59.
[39] A.R. Calabria, C. Weidenfeller, A.R. Jones, H.E. de Vries, E.V. Shusta, Puromycin-purified rat brain microvascular endothelial cell cultures exhibit improved barrier properties in response to glucocorticoid induction, J. Neurochem. 97 (4) (2006) 922–933, https://doi.org/10.1111/j.1471-4159.2006.03793.x.
[40] N. Perriere, P. Demeuse, E. Garcia, A. Regina, M. Debray, J.P. Andreux, P. Couvreur, J.M. Scherrmann, J. Temsamani, P.O. Couraud, M.A. Deli, F. Roux, Puromycin-based purification of rat brain capillary endothelial cell cultures. Effect on the expression of blood-brain barrier-specific properties, J. Neurochem. 93 (2) (2005) 279–289, https://doi.org/10.1111/j.1471-4159.2004.03020.x.
[41] F. Bernard-Patrzynski, M.-A. Lécuyer, I. Puscas, I. Boukhatem, M. Charabati, L. Bourbonnière, C. Ramassamy, G. Leclair, A. Prat, V.G. Roullin, Isolation of endothelial cells, pericytes and astrocytes from mouse brain, PLoS One 14 (12) (2019), e0226302, https://doi.org/10.1371/journal.pone.0226302.
[42] X. Yuan, Q. Wu, P. Wang, Y. Jing, H. Yao, Y. Tang, Z. Li, H. Zhang, R. Xiu, Exosomes derived from pericytes improve microcirculation and protect blood–spinal cord barrier after spinal cord injury in mice, Front. Neurosci. 13 (2019) 319, https://doi.org/10.3389/fnins.2019.00319.
[43] S. Ge, J.S. Pachter, Isolation and culture of microvascular endothelial cells from murine spinal cord, J. Neuroimmunol. 177 (1–2) (2006) 209–214, https://doi.org/10.1016/j.jneuroim.2006.05.012.
[44] M. Toshner, B.J. Dunmore, E.F. McKinney, M. Southwood, P. Caruso, P.D. Upton, J. P. Waters, M.L. Ormiston, J.N. Skepper, G. Nash, A.A. Rana, N.W. Morrell, Transcript analysis reveals a specific hox signature associated with positional identity of human endothelial cells, PLoS One 9 (3) (2014), e91334, https://doi.org/10.1371/journal.pone.0091334.
[45] Y. Molino, F. Jabes, A. Bonnet, N. Gaudin, A. Bernard, P. Benech, M. Khrestchatisky, Gene expression comparison reveals distinct basal expression of hox members and differential tnf-induced response between brain- and spinal cord-derived microvascular endothelial cells, J. Neuroinflammation 13 (1) (2016) 290, https://doi.org/10.1186/s12974-016-0749-6.
[46] J. Karar, A. Maity, Pi3k/akt/mtor pathway in angiogenesis, Front. Mol. Neurosci. 4 (2011) 51, https://doi.org/10.3389/fnmol.2011.00051.
[47] A.R. Ramjaun, K. Hodivala-Dilke, The role of cell adhesion pathways in angiogenesis, Int. J. Biochem. Cell Biol. 41 (3) (2009) 521–530, https://doi.org/10.1016/j.biocel.2008.05.030.
[48] P.D. Thomas, D. Ebert, A. Muruganujan, T. Mushayahama, L.P. Albou, H. Mi, Panther: making genome-scale phylogenetics accessible to all, Protein Sci. 31 (1) (2022) 8–22, https://doi.org/10.1002/pro.4218.
[49] M. D'Angelo, A. Antonosante, V. Castelli, M. Catanesi, N. Moorthy, D. Iannotta, A. Cimini, E. Benedetti, Ppars and energy metabolism adaptation during neurogenesis and neuronal maturation, Int. J. Mol. Sci. 19 (7) (2018) 1869, https://doi.org/10.3390/ijms19071869.
[50] A. Ozkan, A. Bicer, T. Avsar, A. Seker, Z.O. Toktas, S.U. Bozkurt, A.N. Basak, T. Kilic, Temporal expression analysis of angiogenesis-related genes in brain development, Vasc. Cell 4 (1) (2012) 16, https://doi.org/10.1186/2045-824X-4-16.
[51] C. Givens, E. Tzima, Endothelial mechanosignaling: does one sensor fit all? Antioxidants Redox Signal. 25 (7) (2016) 373–388, https://doi.org/10.1089/ars.2015.6493.
[52] L. Liu, Z. You, H. Yu, L. Zhou, H. Zhao, X. Yan, D. Li, B. Wang, L. Zhu, Y. Xu, T. Xia, Y. Shi, C. Huang, W. Hou, Y. Du, Mechanotransduction-modulated fibrotic microniches reveal the contribution of angiogenesis in liver fibrosis, Nat. Mater. 16 (12) (2017) 1252–1261, https://doi.org/10.1038/nmat5024.
[53] R.D. Bartlett, D. Eleftheriadou, R. Evans, D. Choi, J.B. Phillips, Mechanical properties of the spinal cord and brain: comparison with clinical-grade biomaterials for tissue engineering and regenerative medicine, Biomaterials 258 (2020), 120303, https://doi.org/10.1016/j.biomaterials.2020.120303.
[54] W. Xue, C. Fan, B. Chen, Y. Zhao, Z. Xiao, J. Dai, Direct neuronal differentiation of neural stem cells for spinal cord injury repair, Stem Cell. 39 (8) (2021) 1025–1032, https://doi.org/10.1002/stem.3366.
[55] I.M. Pereira, A. Marote, A.J. Salgado, N.A. Silva, Filling the gap: neural stem cells as a promising therapy for spinal cord injury, Pharmaceuticals 12 (2) (2019) 65, https://doi.org/10.3390/ph12020065.
[56] J. Sun, W. Zhou, D. Ma, Y. Yang, Endothelial cells promote neural stem cell proliferation and differentiation associated with vegf activated notch and pten signaling, Dev. Dynam. 239 (9) (2010) 2345–2353, https://doi.org/10.1002/dvdy.22377.
[57] W. Jia, W. Wu, D. Yang, C. Xiao, M. Huang, F. Long, Z. Su, M. Qin, X. Liu, Y.Z. Zhu, Gata4 regulates angiogenesis and persistence of inflammation in rheumatoid arthritis, Cell Death Dis. 9 (5) (2018) 503, https://doi.org/10.1038/s41419-018-0570-5.
[58] K. Xi, Y. Gu, J. Tang, H. Chen, Y. Xu, L. Wu, F. Cai, L. Deng, H. Yang, Q. Shi, W. Cui, L. Chen, Microenvironment-responsive immunoregulatory electrospun fibers for promoting nerve function recovery, Nat. Commun. 11 (1) (2020) 4504, https://doi.org/10.1038/s41467-020-18265-3.
[59] H. Shen, B. Xu, C. Yang, W. Xue, Z. You, X. Wu, D. Ma, D. Shao, K. Leong, J. Dai, A damp-scavenging, il-10-releasing hydrogel promotes neural regeneration and motor function recovery after spinal cord injury, Biomaterials 280 (2022), 121279, https://doi.org/10.1016/j.biomaterials.2021.121279.
[60] C. Li, C. Li, Z. Ma, H. Chen, H. Ruan, L. Deng, J. Wang, W. Cui, Regulated macrophage immune microenvironment in 3d printed scaffolds for bone tumor postoperative treatment, Bioact. Mater. 19 (2023) 474–485, https://doi.org/10.1016/j.bioactmat.2022.04.028.
[61] B.J. Andreone, B. Lacoste, C. Gu, Neuronal and vascular interactions, Annu. Rev. Neurosci. 38 (2015) 25–46, https://doi.org/10.1146/annurev-neuro-071714-033835.
[62] W. Wang, L. Su, Y. Wang, C. Li, F. Ji, J. Jiao, Endothelial cells mediated by ucp2 control the neurogenic-to-astrogenic neural stem cells fate switch during brain development, Adv. Sci. 9 (18) (2022), e2105208, https://doi.org/10.1002/advs.202105208.
[63] W. Li, E.T. Mandeville, V. Duran-Laforet, N. Fukuda, Z. Yu, Y. Zheng, A. Held, J. H. Park, T. Nakano, M. Tanaka, J. Shi, E. Esposito, W. Niu, C. Xing, K. Hayakawa, I. Lizasoain, K. van Leyen, X. Ji, B.J. Wainger, M.A. Moro, E.H. Lo, Endothelial cells regulate astrocyte to neural progenitor cell trans-differentiation in a mouse model of stroke, Nat. Commun. 13 (1) (2022) 7812, https://doi.org/10.1038/s41467-022-35498-6.
[64] J. Wang, Y. Cui, Z. Yu, W. Wang, X. Cheng, W. Ji, S. Guo, Q. Zhou, N. Wu, Y. Chen, Y. Chen, X. Song, H. Jiang, Y. Wang, Y. Lan, B. Zhou, L. Mao, J. Li, H. Yang, W. Guo, X. Yang, Brain endothelial cells maintain lactate homeostasis and control adult hippocampal neurogenesis, Cell Stem Cell 25 (6) (2019) 754–767 e9, https://doi.org/10.1016/j.stem.2019.09.009.
[65] J.R. Vieira, B. Shah, C. Ruiz de Almodovar, Cellular and molecular mechanisms of spinal cord vascularization, Front. Physiol. 11 (2020), 599897, https://doi.org/10.3389/fphys.2020.599897.
[66] K. Tsivelekas, D.S. Evangelopoulos, D. Pallis, I.S. Benetos, S.A. Papadakis, J. Vlamis, S.G. Pneumaticos, Angiogenesis in spinal cord injury: progress and treatment, Cureus 14 (5) (2022), e25475, https://doi.org/10.7759/cureus.25475.
[67] C. Yao, X. Cao, B. Yu, Revascularization after traumatic spinal cord injury, Front. Physiol. 12 (2021), 631500, https://doi.org/10.3389/fphys.2021.631500.
[68] Z. Fan, X. Liao, Y. Tian, X. Xuzhuzi, Y. Nie, A prevascularized nerve conduit based on a stem cell sheet effectively promotes the repair of transected spinal cord injury, Acta Biomater. 101 (2020) 304–313, https://doi.org/10.1016/j.actbio.2019.10.042.
[69] B. Xu, M. Yin, Y. Yang, Y. Zou, W. Liu, L. Qiao, J. Zhang, Z. Wang, Y. Wu, H. Shen, M. Sun, W. Liu, W. Xue, Y. Fan, Q. Zhang, B. Chen, X. Wu, Y. Shi, F. Lu, Y. Zhao, Z. Xiao, J. Dai, Transplantation of neural stem progenitor cells from different sources for severe spinal cord injury repair in rat, Bioact. Mater. 23 (2023) 300–313, https://doi.org/10.1016/j.bioactmat.2022.11.008.
[70] M. Kabat, I. Bobkov, S. Kumar, M. Grumet, Trends in mesenchymal stem cell clinical trials 2004-2018: is efficacy optimal in a narrow dose range? Stem Cells Transl Med 9 (1) (2020) 17–27, https://doi.org/10.1002/sctm.19-0202.
[71] T. Zhou, Y. Zheng, L. Sun, S.R. Badea, Y. Jin, Y. Liu, A.J. Rolfe, H. Sun, X. Wang, Z. Cheng, Z. Huang, N. Zhao, X. Sun, J. Li, J. Fan, C. Lee, T.L. Megraw, W. Wu, G. Wang, Y. Ren, Microvascular endothelial cells engulf myelin debris and promote macrophage recruitment and fibrosis after neural injury, Nat. Neurosci. 22 (3) (2019) 421–435, https://doi.org/10.1038/s41593-018-0324-9.
[72] J. Mai, A. Virtue, J. Shen, H. Wang, X.F. Yang, An evolving new paradigm: endothelial cells–conditional innate immune cells, J. Hematol. Oncol. 6 (2013) 61, https://doi.org/10.1186/1756-8722-6-61.
[73] A. Samakova, A. Gazova, N. Sabova, S. Valaskova, M. Jurikova, J. Kyselovic, The pi3k/akt pathway is associated with angiogenesis, oxidative stress and survival of mesenchymal stem cells in pathophysiologic condition in ischemia, Physiol. Res. 68 (Suppl 2) (2019) S131–S138, https://doi.org/10.33549/physiolres.934345.
[74] C.L. Xiao, W.C. Yin, Y.C. Zhong, J.Q. Luo, L.L. Liu, W.Y. Liu, K. Zhao, The role of pi3k/akt signalling pathway in spinal cord injury, Biomed. Pharmacother. 156 (2022), 113881, https://doi.org/10.1016/j.biopha.2022.113881.
[75] S. Bhowmick, P.M. Abdul-Muneer, Pten blocking stimulates corticospinal and raphespinal axonal regeneration and promotes functional recovery after spinal cord injury, J. Neuropathol. Exp. Neurol. 80 (2) (2021) 169–181, https://doi.org/10.1093/jnen/nlaa147.